

# Beam Dynamics in $\mathcal{PT}$ Symmetric Optical Lattices

K. G. Makris, R. El-Ganainy, and D. N. Christodoulides

*College of Optics & Photonics-CREOL, University of Central Florida, Orlando, Florida 32816, USA*

Z. H. Musslimani

*Department of Mathematics, Florida State University, Tallahassee, Florida 32306-4510, USA*

(Received 5 June 2007; revised manuscript received 9 October 2007; published 13 March 2008)

The possibility of parity-time ( $\mathcal{PT}$ ) symmetric periodic potentials is investigated within the context of optics. Beam dynamics in this new type of optical structures is examined in detail for both one- and two-dimensional lattice geometries. It is shown that  $\mathcal{PT}$  periodic structures can exhibit unique characteristics stemming from the nonorthogonality of the associated Floquet-Bloch modes. Some of these features include double refraction, power oscillations, and eigenfunction unfolding as well as nonreciprocal diffraction patterns.

DOI: [10.1103/PhysRevLett.100.103904](https://doi.org/10.1103/PhysRevLett.100.103904)

PACS numbers: 42.25.Bs, 11.30.Er, 42.82.Et

Over the last few years a new concept has been proposed in an attempt to extend the framework of quantum mechanics into the complex domain. In 1998, Bender *et al.* found [1] that it is in fact possible even for non-Hermitian Hamiltonians to exhibit entirely real eigenvalue spectra as long as they respect parity-time requirements or  $\mathcal{PT}$  symmetry [2–4]. This fascinating result appears to be counter-intuitive since it implies that all the eigenmodes of a pseudo-Hermitian Hamiltonian [5] (bound as well as radiation states) are only associated with real eigenenergies. Another intriguing characteristic is related to spontaneous  $\mathcal{PT}$  symmetry-breaking beyond which this class of systems can undergo an abrupt *phase transition* [1]. In particular, above this critical threshold, the system loses its  $\mathcal{PT}$  property and as a result some of the eigenvalues become complex. The notion of  $\mathcal{PT}$  symmetry is now extensively considered in diverse areas of physics including, for example, quantum field theories [2], non-Hermitian Anderson models, complex Lie algebras, and lattice QCD theories just to mention a few [6]. It is worth mentioning that, even before the  $\mathcal{PT}$  concept was introduced, wave scattering from complex periodic potentials has been considered at both the theoretical [7] and experimental front [8].

In general, a Hamiltonian is  $\mathcal{PT}$  symmetric provided that all its eigenfunctions are simultaneously eigenfunctions of  $\mathcal{PT}$  operator [2]. Here the action of the parity operator  $\hat{P}$  is defined by the relations  $\hat{p} \rightarrow -\hat{p}$ ,  $\hat{x} \rightarrow -\hat{x}$  while that of the time operator  $\hat{T}$  by  $\hat{p} \rightarrow -\hat{p}$ ,  $\hat{x} \rightarrow \hat{x}$ ,  $i \rightarrow -i$ , where  $\hat{p}$ ,  $\hat{x}$  denote momentum and position operators, respectively. In operator form, the normalized Schrödinger evolution equation ( $\hbar = m = 1$ ) is given by  $i\Psi_t = \hat{H}\Psi$ , where  $\hat{H} = \hat{p}^2/2 + V(\hat{x})$  and  $\hat{p} \rightarrow -i\partial/\partial x$  [9]. Given that the  $\hat{T}$  operation corresponds to a time reversal, i.e.,  $\hat{T}\hat{H} = \hat{p}^2/2 + V^*(x)$ , then one can deduce that  $\hat{H}\hat{P}\hat{T} = \hat{p}^2/2 + V(x)$  and  $\hat{P}\hat{T}\hat{H} = \hat{p}^2/2 + V^*(-x)$ . From the above considerations one finds that a necessary condition for a

Hamiltonian to be  $\mathcal{PT}$  symmetric is  $V(x) = V^*(-x)$ . This last relation indicates that parity-time symmetry requires that the real part of the complex potential involved must be an even function of position whereas the imaginary component should be odd.

While the implications of  $\mathcal{PT}$  symmetry in the above mentioned fields are still under consideration, as we will show some of these basic concepts can be realized in optics. This can be achieved through a judicious design that involves a combination of optical gain or loss regions and the process of index guiding. Of particular importance is to explore the properties of periodic  $\mathcal{PT}$  symmetric lattices as this may lead to pseudo-Hermitian synthetic materials. Quite recently, conventional optical array structures (based on real potentials) have received considerable attention and have been examined in several systems including semiconductors, glasses, quadratic and photorefractive materials, and liquid crystals [10]. Given that even a single  $\mathcal{PT}$  cell can exhibit unconventional features, one may naturally ask what new behavior and properties could be expected from parity-time symmetric optical lattices.

In this Letter we investigate optical beam dynamics in complex  $\mathcal{PT}$  arrays. The unusual band structure properties of these periodic systems is systematically examined in both one- and two-dimensional geometries. We find that above the phase-transition point, bands can merge forming loops or closed ovals (attached to a 2D membrane) within the Brillouin zone and the Floquet-Bloch (FB) modes are substantially altered. Our analysis indicates that under wide beam excitation, interesting diffraction patterns emerge such as “double refraction” and power oscillations due to eigenfunction unfolding. We show that this dynamics is a direct outcome of mode skewness or nonorthogonality. The nonreciprocal characteristics of these  $\mathcal{PT}$  arrays are also discussed.

In optics, several classical processes are known to obey a Schrödinger-like equation. Perhaps the most widely known

physical effects associated with this evolution equation are those of spatial diffraction and temporal dispersion [11]. Here we will primarily explore the diffraction dynamics of optical beams and waves in  $\mathcal{PT}$  symmetric potentials in the spatial domain. Along these lines, let us consider a complex parity-time potential. In this case, the complex refractive index of the system is described by  $n = n_0 + n_R(x) + in_I(x)$ , where  $n_0$  is the background refractive index,  $n_R(x)$  is the real index profile of the lattice, and  $n_I(x)$  represents the gain or loss periodic distribution of the structure [in practice  $n_0 \gg n_{R,I}(x)$ ]. Under these conditions, the electric field envelope  $U$  of the beam obeys the paraxial equation of diffraction:  $iU_z + (2k_0n_0)^{-1}U_{xx} + k_0[n_R(x) + in_I(x)]U = 0$ , where  $z$  is the propagation distance,  $x$  is the transverse coordinate, and  $k_0 = 2\pi/\lambda_0$  with  $\lambda_0$  being the light wavelength. We note that this latter equation is formally analogous to a Schrödinger equation. In an array arrangement  $n_{R,I}(x + D) = n_{R,I}(x)$ , where  $D$  represents the lattice period. From our previous discussion, this complex potential is  $\mathcal{PT}$  symmetric provided that its real part or refractive index profile is even, i.e.,  $n_R(x) = n_R(-x)$ , while the imaginary component  $n_I(x)$  (that is loss or gain) is odd. From a physical perspective such  $\mathcal{PT}$  symmetric lattices can be realized in the visible and in the long wavelength regime ( $0.5 \mu\text{m} < \lambda_0 < 1.6 \mu\text{m}$ ) using a periodic index modulation of the order of  $\Delta n_R^{\text{max}} \approx 10^{-3}$  with  $D \approx 10\text{--}20 \mu\text{m}$  (similar to those encountered in real arrays [10]) provided that the maximum gain or loss values are approximately  $g = -\alpha \approx 30 \text{ cm}^{-1}$  or  $\Delta n_I^{\text{max}} \approx 5 \times 10^{-4}$ . Such gain or loss coefficients can be realistically obtained from quantum well lasers or photorefractive structures through two-wave mixing [11]. By introducing the following scaled quantities,  $\xi = z/(2k_0n_0x_0^2)$ ,  $\eta = x/x_0$ ,  $V(\eta) = 2k_0^2n_0x_0^2(n_R + in_I)$ , (where  $x_0$  is an arbitrary scaling factor) the normalized equation of diffraction can now be expressed in the form:

$$i \frac{\partial U}{\partial \xi} + \frac{\partial^2 U}{\partial \eta^2} + V(\eta)U = 0. \quad (1)$$

To understand the properties of a periodic  $\mathcal{PT}$  structure we must first analyze its corresponding band structure. In particular, we seek solutions of the form  $\phi_{kn}(\eta) \times \exp(i\beta_{kn}\xi)$ , where  $\phi_{kn}(\eta)$  is the  $n$ -band Floquet-Bloch mode at Bloch momentum  $k$ , and  $\beta_{kn}$  is the associated eigenvalue or propagation constant. For illustration purposes we assume the periodic  $\mathcal{PT}$  potential  $V(\eta) = A[\cos^2(\eta) + iV_0 \sin(2\eta)]$ , ( $A = 4$ ) with period  $D = \pi x_0$  for both real and imaginary component [shown schematically in Fig. 1(a)]. We stress that the requirement  $V(\eta) = V^*(-\eta)$  satisfied by this potential is a necessary but not a sufficient condition for the eigenvalue spectrum to be real. By using spectral techniques we numerically identify the  $\mathcal{PT}$  threshold ( $V_0^{\text{th}}$ ), below which all the propagation eigenvalues for every band and every Bloch wave number  $k$  are real. Above this  $\mathcal{PT}$  threshold, an abrupt phase transition occurs because of spontaneous symmetry break-

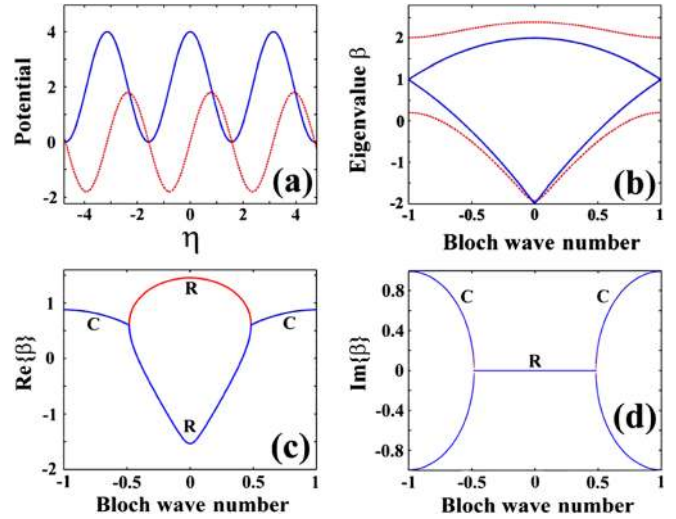


FIG. 1 (color online). (a) Real part (solid line) and imaginary component (dotted line) of the  $\mathcal{PT}$  potential  $V(\eta) = 4[\cos^2(\eta) + iV_0 \sin(2\eta)]$ ; (b) corresponding band structure for  $V_0 = 0.2$  (dotted line) and  $V_0 = 0.5$  (solid line). (c), (d) Real and imaginary part of the double-valued band for  $V_0 = 0.7$ , respectively, resulting from the merging of the two first bands.

ing and as a result the spectrum is partially complex. This happens in spite of the fact that  $V(\eta) = V^*(-\eta)$  is still satisfied. For the particular potential considered here we find that  $V_0^{\text{th}} = 0.5$ . More specifically, for  $V_0 < 0.5$ , the band structure is entirely real while for  $V_0 > 0.5$  it becomes complex (starting from the lowest bands). Figure 1(b) depicts the first two bands of this potential for two cases, i.e., when  $V_0 = 0.2$  and  $0.5$ . Note that below  $V_0^{\text{th}}$  all the forbidden gaps are open whereas at the threshold  $V_0^{\text{th}} = 0.5$  some band gaps at the edges of the Brillouin zone close (no gaps exist at  $k = \pm 1$ ) as shown in Fig. 1(b). On the other hand, when  $V_0$  exceeds this critical value these two same bands start to merge together and in doing so they form oval-like structures with a related complex spectrum. The real as well as the imaginary parts of such a double-valued band when  $V_0 = 0.7$  are depicted in Figs. 1(c) and 1(d), respectively. These figures show that the propagation eigenvalues are entirely real in the double-valued regions (oval  $R$  regions) while along the overlapped sections ( $C$  lines) happen to be complex conjugate. Some of these aspects associated with the real part of these bands were also discussed by Bender *et al.* [12] for pseudo-Hermitian periodic potentials having zero  $\mathcal{PT}$  threshold (purely imaginary potentials with  $V_0^{\text{th}} = 0$ ).

Relevant to our previous discussion is the structure and properties of the corresponding Floquet-Bloch modes for  $\mathcal{PT}$  symmetric potentials. Unlike real potentials, the eigenfunctions have no zero nodes at  $k = \pm 1$  (edge of the Brillouin zone) [12]. In addition, at  $k = \pm 1$  in the complex conjugate part, these functions are shifted with respect to their potentials. We emphasize that the above unexpected modal structure is a direct consequence of the nonorthogonality of the related Floquet-Bloch func-

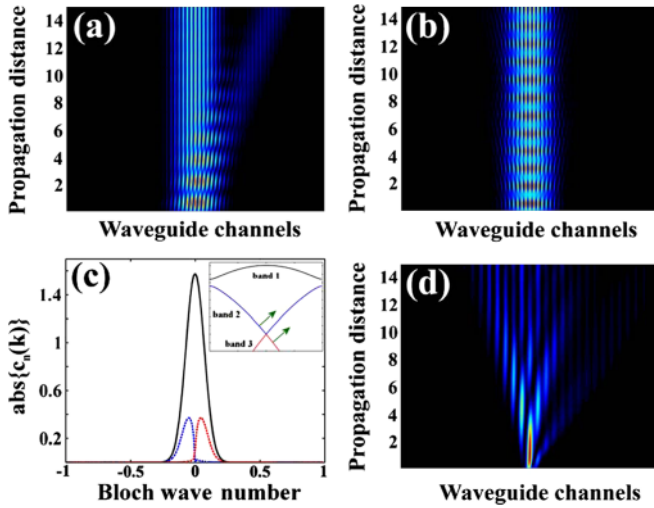


FIG. 2 (color online). Intensity evolution of a broad optical beam under normal incidence when (a)  $V_0 = 0.49$ , (b)  $V_0 = 0$ . (c) depicts the FB decomposition of the input in (a) for the first three bands (solid black line—1st, left dashed blue line—2nd, right dashed red line—3rd), and the inset shows the corresponding band structure. (d) Single channel excitation of this same lattice when  $V_0 = 0.49$ .

tions. In particular, the usual orthogonality condition  $\int_{-\infty}^{+\infty} \phi_{k'm}^*(\eta) \phi_{kn}(\eta) d\eta = \delta_{nm} \delta(k - k')$  (that holds in real crystals) is no longer applicable in  $\mathcal{PT}$  symmetric lattices. This skewness of the modes [13] is an inherent characteristic of  $\mathcal{PT}$  symmetric periodic potentials and has a profound effect on their algebra.

The most interesting aspects associated with  $\mathcal{PT}$  symmetric lattices are revealed during dynamic beam evolution. Figure 2(a) illustrates the intensity distribution during propagation when the  $\mathcal{PT}$  array  $V(\eta) = A[\cos^2(\eta) + iV_0 \sin(2\eta)]$  (with  $V_0 = 0.49$ ,  $A = 4$ ) is excited by a wide optical beam at normal incidence. Figure 2(b) on the other hand shows this same process in the real version of this lattice ( $V_0 = 0$ ) under the same input conditions. These two figures indicate that there is a marked difference between these two regimes. In the  $\mathcal{PT}$  array the beam splits in two and double refraction occurs at an angle of  $\sim 1^\circ$  after 3 cm of propagation when  $D = 20 \mu\text{m}$ ,  $g = 35 \text{ cm}^{-1}$ ,  $\Delta n_R^{\text{max}} = 10^{-3}$ . In order to explain this behavior we project the input field on an orthogonalized Floquet-Bloch base of the complex array; e.g., we write  $U(\eta, \xi) = \int_{-1}^1 \sum_{n=1}^{+\infty} c_n(k) \tilde{\phi}_{kn}(\eta) \exp(i\beta_{kn}\xi) dk$ , where  $c_n(k)$  represent the mode occupancy coefficients in band  $n$  and at Bloch momentum  $k$ . This decomposition was accomplished by devising a new orthogonal basis suitable for  $\mathcal{PT}$  periodic potentials. In this case, the projections are facilitated by:

$$\int_{-\infty}^{+\infty} \tilde{\phi}_{-k'm}^*(-\eta) \tilde{\phi}_{kn}(\eta) d\eta = d_{kn} \delta_{nm} \delta(k - k'), \quad (2)$$

where  $d_{kn} = \{\pm 1\}$  and  $\tilde{\phi}_{kn} = \phi_{kn} / [\int_{-\infty}^{+\infty} \phi_{-kn}^*(-\eta) \phi_{kn}(\eta) d\eta]^{1/2}$ . Unlike real lattices, in these pseudo-

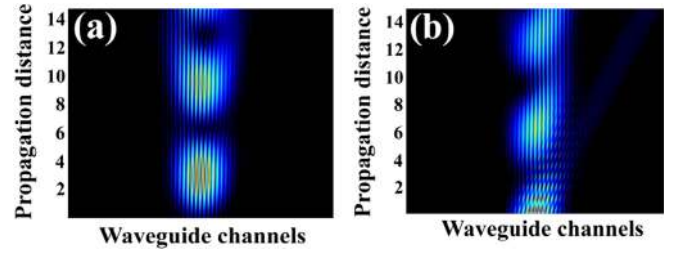


FIG. 3 (color online). Intensity evolution of wide beams exciting a  $\mathcal{PT}$  lattice at angle  $\theta$  when  $V_0 = 0.45$ ,  $A = 4$  and (a)  $\theta = 2^\circ$ , (b)  $\theta = -2^\circ$ .

Hermitian structures, the inner product is taken by reflecting both the spatial coordinate and the Bloch momentum itself. Consequently, the modal coefficients can be obtained from  $c_n(k) = d_{kn} \int_{-\infty}^{+\infty} \tilde{\phi}_{-kn}^*(-\eta) G(\eta) d\eta$ , where  $G(\eta)$  is the input beam profile. Figure 2(c) depicts the  $|c_n(k)|$  occupancy (among bands) corresponding to the input used in Fig. 2(a). This result clearly shows that this distribution is asymmetric in  $k$  space especially in the second and third band while in the first band it is almost symmetric. This asymmetry is attributed to the skewness of the FB modes. Keeping in mind that the beam components will propagate along the gradient  $\nabla_k(\beta)$ , one can then explain from Fig. 2(c) why the double refraction process occurs towards the right. Intuitively this can be understood given that the  $\mathcal{PT}$  periodic structure involves gain or loss dipoles, thus promoting energy flow from left to right. Another feature associated with Fig. 2(a) is power oscillation. Even though this lattice is operated below the  $\mathcal{PT}$  threshold value and hence the entire spectrum is real, what is conserved here is the quasipower [14], e.g.,  $Q = \int_{-\infty}^{+\infty} U(\eta, \xi) U^*(-\eta, \xi) d\eta$  as opposed to the actual power itself  $P = \int_{-\infty}^{+\infty} |U(\eta, \xi)|^2 d\eta$ , which oscillates during propagation. These power oscillations are due the unfolding of the nonorthogonal FB modes. This unfolding process becomes even more pronounced under narrow-beam excitation conditions where secondary emissions can be observed during discrete diffraction as shown in Fig. 2(d).

Another direct consequence of this modal “skewness” is nonreciprocity. Figure 3 shows beam propagation in a  $\mathcal{PT}$  lattice when excited by a wide beam at  $\pm\theta$  angle of incidence (in this case  $2^\circ$ ). Note that the two diffraction

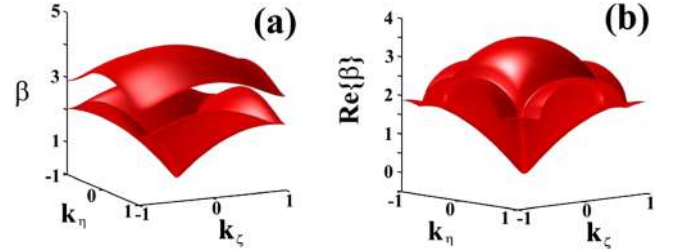


FIG. 4 (color online). Two-dimensional band structures associated with  $V(\eta, \xi)$ , when  $A = 4$  and (a)  $V_0 = 0.45$  and (b)  $V_0 = 0.6$ .



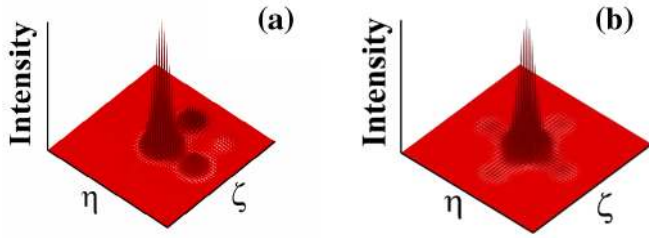


FIG. 5 (color online). Output intensity profiles: (a) for the 2D  $\mathcal{PT}$  potential  $V(\eta, \zeta)$  with  $V_0 = 0.45$  and (b) for the corresponding real lattice  $V_0 = 0$ .

patterns are different and hence, light propagating in  $\mathcal{PT}$  symmetric arrays can distinguish left from right. This is another general property of such pseudo-Hermitian optical systems.

These effects can also be considered in two-dimensional configurations provided that the optical potential satisfies  $V(\eta, \zeta) = V^*(-\eta, -\zeta)$  in the wave equation  $iU_\eta + U_{\eta\eta} + U_{\zeta\zeta} + V(\eta, \zeta)U = 0$ . In the following examples we consider the complex  $\mathcal{PT}$  symmetric potential  $V(\eta, \zeta) = A\{\cos^2(\eta) + \cos^2(\zeta) + iV_0[\sin(2\eta) + \sin(2\zeta)]\}$ , with  $(A = 4)$ . Numerical analysis reveals that the threshold in this separable 2D case is again  $V_0^{\text{th}} = 0.5$ . The real part of the band structure corresponding to this potential is shown in Figs. 4 for two cases, below and above threshold ( $V_0 = 0.45$  and  $V_0 = 0.6$ ). Again below threshold the eigenvalue spectrum is real while at  $V_0^{\text{th}} = 0.5$  the two bands collide at their  $M$  points at the edges of the Brillouin zone, Fig. 4(a). On the other hand, above the phase-transition point (at  $V_0 = 0.6$ ) the first two bands merge thus forming a two-dimensional oval double-valued surface (upon which all the propagation constants are real) attached to a 2D membrane where the complex conjugate eigenvalues reside [see Fig. 4(b)]. The double refraction process in such 2D pseudo-Hermitian structures ( $V_0 = 0.45$ ) is shown in Fig. 5(a) when the system is excited by a normally incident wide 2D Gaussian beam. As opposed to the familiar 2D discrete diffraction pattern occurring in real lattices [Fig. 5(b) with  $V_0 = 0$ ], in the  $\mathcal{PT}$  case, two significant secondary lobes are produced only in the first quadrant. This is of course another manifestation of parity-time symmetry.

In conclusion, we have demonstrated that  $\mathcal{PT}$  symmetric periodic potentials can exhibit new behavior in optics. Beam dynamics in such structures reveal that double refraction, power oscillations, and secondary emissions are possible. The existence of abrupt phase transitions, as well

as the associated band structure of  $\mathcal{PT}$  lattices in both one and two geometries, was also examined in detail. These issues are of direct relevance to other configurations such as those associated with coupled and nonlinear  $\mathcal{PT}$  systems [15].

- 
- [1] C.M. Bender and S. Boettcher, Phys. Rev. Lett. **80**, 5243 (1998).
  - [2] C.M. Bender, D.C. Brody, and H.F. Jones, Phys. Rev. Lett. **89**, 270401 (2002); C.M. Bender, Am. J. Phys. **71**, 1095 (2003); Z. Ahmed, Phys. Lett. A **282**, 343 (2001).
  - [3] C.M. Bender, D.C. Brody, H.F. Jones, and B.K. Meister, Phys. Rev. Lett. **98**, 040403 (2007).
  - [4] M. Znojil, Phys. Lett. A **285**, 7 (2001); A. Mostafazadeh, J. Math. Phys. (N.Y.) **43**, 3944 (2002).
  - [5] N. Moiseyev, Phys. Rep. **302**, 212 (1998); N. Moiseyev and S. Friedland, Phys. Rev. A **22**, 618 (1980).
  - [6] I.Y. Goldsheid and B.A. Khoruzhenko, Phys. Rev. Lett. **80**, 2897 (1998); B. Bagchi and C. Quesne, Phys. Lett. A **273**, 285 (2000); H. Markum, R. Pullirsch, and T. Wettig, Phys. Rev. Lett. **83**, 484 (1999).
  - [7] M.V. Berry and H.J. O'Dell, J. Phys. A **31**, 2093 (1998); M.V. Berry, J. Phys. A **31**, 3493 (1998).
  - [8] D.O. Chudesnikov and V.P. Yakovlev, Laser Phys. **1**, 110 (1991); M.K. Oberthaler *et al.*, Phys. Rev. Lett. **77**, 4980 (1996); C. Keller *et al.*, Phys. Rev. Lett. **79**, 3327 (1997).
  - [9] R. Shankar, *Principles of Quantum Mechanics* (Plenum Press, New York, 1994).
  - [10] D.N. Christodoulides, F. Lederer, and Y. Silberberg, Nature (London) **424**, 817 (2003).
  - [11] A. Yariv, *Optical Electronics in Modern Communications* (Oxford University Press, Oxford, 1997); P. Yeh, *Introduction to Photorefractive Nonlinear Optics*, Wiley Series in Pure and Applied Optics (Wiley, New York, 2001).
  - [12] C.M. Bender, G.V. Dunne, and P.N. Meisinger, Phys. Lett. A **252**, 272 (1999); H.F. Jones, Phys. Lett. A **262**, 242 (1999); Z. Ahmed, Phys. Lett. A **286**, 231 (2001); J.K. Boyd, J. Math. Phys. (N.Y.) **42**, 15 (2001).
  - [13] Yuh-Jen Cheng, C.G. Fanning, and A.E. Siegman, Phys. Rev. Lett. **77**, 627 (1996); A.M. van der Lee, N.J. van Druten, A.L. Mieremet, M.A. van Eijkelenborg, A.M. Lindberg, M.P. van Exter, and J.P. Woerdman, Phys. Rev. Lett. **79**, 4357 (1997).
  - [14] B. Bagchi, C. Quesne, and M. Znojil, Mod. Phys. Lett. A **16**, 2047 (2001).
  - [15] R. El-Ganainy, K.G. Makris, D.N. Christodoulides, and Z.H. Musslimani, Opt. Lett. **32**, 2632 (2007); Z.H. Musslimani, K.G. Makris, R. El-Ganainy, and D.N. Christodoulides, Phys. Rev. Lett. **100**, 030402 (2008).